

RESEARCH PAPER

## Evaluation of Nanoparticle Tantalum Pentoxide Coatings on Nickel Titanium Alloy for Orthodontic Archwires (in Vitro Study)

Abeer Basim Mahmood<sup>1</sup>, Mohammed K. Khalaf<sup>2\*</sup>, Akram Faisal Alhuwaizi<sup>1</sup>

<sup>1</sup> Orthodontic Department, College of Dentistry, University of Baghdad, Baghdad, Iraq

<sup>2</sup> Center of Applied Physics, Directorate of Materials Research, Ministry of Higher Education and Scientific Research /Science and Technology, Baghdad, Iraq

### ARTICLE INFO

#### Article History:

Received 19 January 2023

Accepted 27 March 2023

Published 01 April 2023

#### Keywords:

Biocompatibility

Corrosion

DC Sputtering

Nickel/Titanium

Ta<sub>2</sub>O<sub>5</sub> coatings

### ABSTRACT

Tantalum pentoxide (Ta<sub>2</sub>O<sub>5</sub>) thin films were deposited on Nickel Titanium Alloy (NiTi) substrates using DC magnetron reactive sputtering at a low temperature of about 100°C, with a power input of 50 Watts. Advanced techniques such as X-ray diffraction, Atomic Force Microscopy (AFM), and Scanning Electron Microscopy (SEM) were employed to analyze the Ta<sub>2</sub>O<sub>5</sub> coatings. The results revealed that these coatings displayed remarkable uniformity, with extremely low surface roughness (only 2.75 nanometers) and particles in the 15-30 nanometer range. Microhardness was also measured via nanoindentation. Beyond structural and morphological attributes, the study explored the suitability of Ta<sub>2</sub>O<sub>5</sub>-coated NiTi alloys for biomedical applications, particularly orthodontic archwires. Assessments covered corrosion resistance, biocompatibility, and nickel ion release in artificial saliva (AS) and simulated body fluid (SBF) solutions. The findings demonstrated enhanced electrochemical behavior, significantly improved corrosion resistance, enhanced biocompatibility, and lower nickel ion release for Ta<sub>2</sub>O<sub>5</sub>-coated NiTi alloys than uncoated ones. These benefits are attributed to the improved cohesiveness of the Ta<sub>2</sub>O<sub>5</sub> coatings. In summary, sputtering Ta<sub>2</sub>O<sub>5</sub> films onto NiTi alloys offers a promising avenue for biomedical surface modification. The exceptional uniformity and improved properties of Ta<sub>2</sub>O<sub>5</sub>-coated NiTi alloys position them as valuable candidates for orthodontic archwires and other biomedical devices, showcasing the potential of this method in advancing medical and dental technology materials.

### How to cite this article

Mahmood A B., Khalaf M K., Alhuwaizi A F. Evaluation of Nanoparticle Tantalum Pentoxide Coatings on Nickel Titanium Alloy for Orthodontic Archwires (in Vitro Study). J Nanostruct, 2023; 13(2):462-470. DOI: 10.22052/JNS.2023.02.016

### INTRODUCTION

The quest for biomaterials with tailored characteristics to modulate biological responses is paramount in orthopedic and dental implants. The surface properties of these materials play a pivotal role in dictating their biological interactions. As a

result, coatings imbued with biologically relevant attributes, such as osteoinductivity, offer intriguing avenues for customizing the surfaces of diverse bulk materials. Metal oxide coatings like TiO<sub>2</sub>, ZrO<sub>2</sub>, Nb<sub>2</sub>O<sub>5</sub>, and Ta<sub>2</sub>O<sub>5</sub> have been proposed to enhance the performance of orthopedic and dental

\* Corresponding Author Email: [mohammedkhkh@yahoo.com](mailto:mohammedkhkh@yahoo.com)



implants [1]. Among these metal oxide coatings, tantalum pentoxide ( $Ta_2O_5$ ) thin films have garnered significant attention due to their wide-ranging applications, encompassing solar cells, sensors, photocatalysis, and surface modification for biomedical alloys. Numerous studies have delved into the intricate relationships between experimental parameters, film characteristics, and precise control of the deposition process. Several synthesis techniques have been explored in this pursuit, including sol-gel [2], electron beam evaporation [3,4], bias-assisted cathodic arc deposition [5], oxidation processes [6,7], atomic layer deposition [8,9], electrophoretic deposition [10], physical vapor deposition (PVD) [11,12], pulsed laser deposition (PLD) [13], plasma source ion implantation [14], DC magnetron sputtering [15,16], medium-frequency magnetron sputtering [17,18], and RF magnetron sputtering [19,20]. Among these methods, DC magnetron sputtering is a particularly advantageous choice. It offers flexibility in selecting and fine-tuning deposition conditions while maintaining low substrate temperatures. This technique ensures the uniform delivery of material to the growing surface layer, facilitating the construction of substantial structures [19].

In parallel, there is a growing recognition of the potential for enhancing the medical performance of NiTi implants, stents, and catheters by applying functional anti-corrosion coatings. The deposition of coatings containing tantalum (Ta) and its oxides on metal implants can significantly enhance mechanical properties, bolster corrosion resistance, and improve chemical inertness and biocompatibility [1]. In this study, we journeyed to deposit  $Ta_2O_5$  coatings onto NiTi alloy surfaces using the DC reactive magnetron sputtering

method. Our goal was to explore the potential applications of these coatings in the biomedical field, focusing on their impact on the performance of NiTi alloy implants.

**MATERIALS AND METHODS**

DC magnetron reactive a sputtering (CRC-600 system, Torr Inc., USA) method utilized to produce  $Ta_2O_5$  thin films on NiTi and glass substrates with working conditions as shown in table (1) where P1 is the base vacuum pressure and P2 is the vacuum sputtering chamber of working argon/oxygen mixture, T is the temperature of the substrate which was in the range (~100°C). The target type is Ta of 99.99% in dimension of D =5cm and thickness of 3mm. This work measures the  $Ta_2O_5$  thin film thickness using an optical interferometer method. The substrates were set 10 cm away from the target. Pumped down to  $1 \times 10^{-5}$  mbar was the sputtering chamber pressure. Acetone and ethanol were sonicated onto the substrates for six minutes to clean them. The substrates were etched in argon at a pressure of 7.45 10-3 mbar before deposition to remove any potential contaminants. The films were deposited at a working pressure of about  $1 \times 10^{-2}$  mbar, the applied power was 50 Watt, and the sputtering time was 120 min. The XRD measurements were performed using a Shimadzu X-ray diffractometer with a wavelength of 1.54056Å. Measurements for phase detection using X-ray diffraction were made. The surface morphology of the sample will be evaluated using a field emission scan electron microscope (FESEM): Hitachi (S-4160), the magnification power continuously from 10,00kx to 50,00kx. The elemental composition of a layer of coated  $TiO_2$  was determined using an Energy-Dispersive X-ray Spectrometer (EDXS) unit

Table 1. The working conditions of  $Ta_2O_5$  thin films prepared via dc sputtering method

dc sputtering power	50Watt
Base pressure P1	$1 \times 10^{-5}$ mbar
Working pressure P2	$1 \times 10^{-2}$ mbar
Working gas	Ar/O <sub>2</sub> (%20)
Electrode spacing	10cm
Substrate temperature Ts	100°C
Sputtering time	120 min



interfaced with an FESEM. The release of nickel ions was determined by measuring the nickel ion content in the Artificial Saliva (AS) solution. The samples were statically immersed in 100 ml of AS solutions in separate containers for 14 days. A graphite-furnace atomic absorption spectrometry (GFAAS) (AA6501F, Shimadzu, Japan) measured the nickel ion release release.

## RESULTS AND DISCUSSIONS

### Structural Analysis

To confirm the successful coating of NiTi samples with Ta<sub>2</sub>O<sub>5</sub> thin film, we conducted an X-ray diffraction (XRD) analysis. Fig. 1 illustrates the XRD pattern for uncoated and Ta<sub>2</sub>O<sub>5</sub>-coated NiTi substrates, with a consistent sputtering power 50W and a film thickness of 118.6 nm. In the XRD patterns, only the reflections associated with the atomic plane (105) of the Ta<sub>2</sub>O<sub>5</sub> phase, as per the ICDD crystallographic card No. 21-1198, were observed across all experiments, with 2θ values at 27.319 degrees. Notably, the results indicated that the films deposited at a substrate temperature of 100°C exhibited an amorphous phase. However, the crystallinity of the Ta<sub>2</sub>O<sub>5</sub> thin films was significantly enhanced to the orthorhombic phase (β-Ta<sub>2</sub>O<sub>5</sub>) through a crucial thermal annealing process. This transformation underscores the importance of thermal treatment in achieving the desired crystalline structure for Ta<sub>2</sub>O<sub>5</sub> thin films.

### Surface Morphology

Quantitatively assessing the dimensional surface roughness of nanoparticles and visualizing the nano-texture on the film coating's surface is conveniently achieved through atomic force microscope (AFM) analysis. Various parameters are employed to characterize the surface profile, including the average roughness (Ra), the root mean square roughness (Rq), and the average grain size of the coating layer. The grain size is a critical parameter for understanding growth conditions, as it directly influences essential recording properties like aerial density and thermal stability [21].

Fig. 2 presents both a histogram and three-dimensional (3D) AFM images of the Ta<sub>2</sub>O<sub>5</sub> film coating. These images exhibit distinct light and dark regions, with brightness serving as an indicator of the thin film's vertical profile. Light regions correspond to elevated points, while dark areas represent depressions. This visualization confirms the uniformity of the thin layer, demonstrating that the substrate surface is effectively covered with nearly evenly distributed grains. From the AFM images, we derived quantitative values for surface characteristics: the average roughness (Ra) measures at 2.75nm, the root mean square roughness (Rq) at 4.13nm, and the average grain size is determined to be 118.9nm. It's noteworthy that roughness tends to increase with larger grain sizes. However, in the case of thin layers with specific compositions, different outcomes may

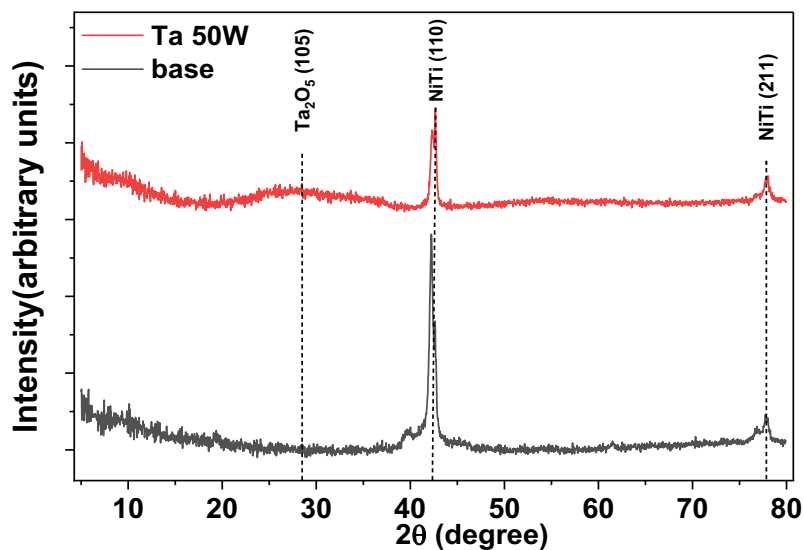


Fig. 1. XRD patterns of uncoated and Ta<sub>2</sub>O<sub>5</sub>-coated NiTi samples.

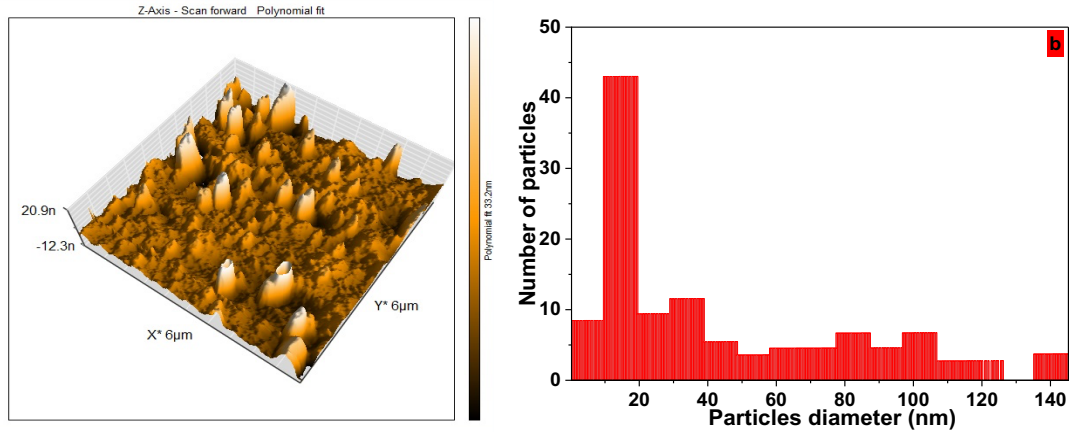


Fig. 2. 3D- AFM images and histogram of Ta<sub>2</sub>O<sub>5</sub> nanoparticles coating layer deposited at sputtering power of 50Watt

arise depending on factors such as the material type, deposition method, conditions (including temperature and substrate choice), and potential chemical reactions during the deposition process [22].

The Ta<sub>2</sub>O<sub>5</sub> thin film generated with a lower power setting of 50 Watts exhibits notable grains with distinct orientations, as evidenced in Fig.2. These morphological characteristics are a consequence of increased surface mobility of adatoms, a crucial

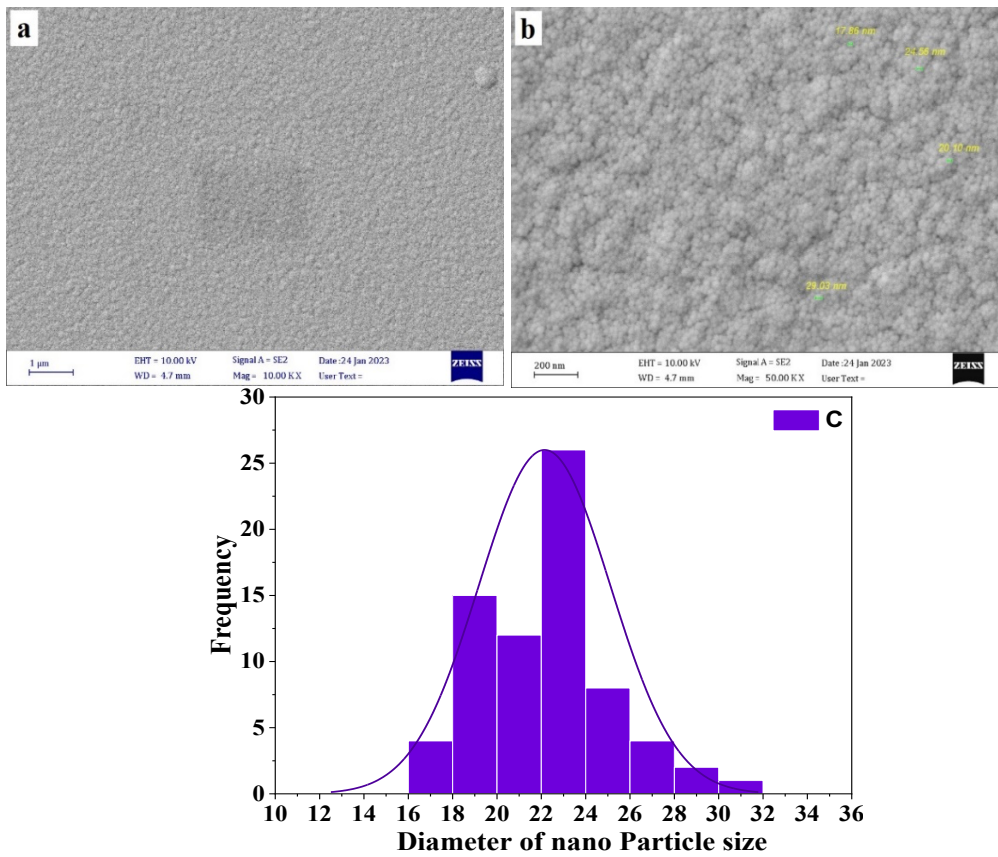


Fig. 3. (a and b) FESEM image at different magnifications of the Ta<sub>2</sub>O<sub>5</sub> nanoparticle coating layer deposited at 50 W, (c) average diameters of the granular distribution.

factor in forming continuous thin layers.

Fig. 3 presents FESEM (Field Emission Scanning Electron Microscope) images of the Ta<sub>2</sub>O<sub>5</sub> thin coating layer deposited on NiTi samples, captured at magnification powers of 10.00Kx and 50.00Kx. These images vividly illustrate the Ta<sub>2</sub>O<sub>5</sub> nanoparticles within the coating layer, which were deposited at a sputtering power of 50 watts. Notably, these nanoparticles exhibit a uniform and homogeneous distribution across the surface. The as-deposited samples appear notably smooth, aligning with the findings from Huang's paper and reaffirming the amorphous nature of the Ta<sub>2</sub>O<sub>5</sub> thin films [23].

In terms of particle size, the Ta<sub>2</sub>O<sub>5</sub> nanoparticles within the coating layer deposited at 50 watts fall within the range of 15-30 nanometers. This range is consistent with existing knowledge that the sputtering power employed during DC magnetron reactive sputtering significantly influences the quality and growth rate of thin films. Furthermore, the particle size of the thin film coatings is recognized to be directly proportional to their crystallinity [24,25].

*Microhardness Measurements*

The choice of Ta<sub>2</sub>O<sub>5</sub> coatings was motivated by their exceptional adhesion to NiTi and their resistance to corrosion, while still maintaining a certain degree of hardness and ductility. Ta<sub>2</sub>O<sub>5</sub> coatings possess remarkable stiffness, and they directly bear the load applied to the NiTi substrate, as documented in previous studies [26]. When subjected to a load, the substrate undergoes elastic deformation, and this phenomenon allows us to examine the relationship between load

and hardness. These findings revealed a complex interplay between substrate and coating hardness, with implications for the overall coating quality.

Numerous tests were conducted on each sample, and the average hardness values were determined. The assessment of precise hardness in the sampled areas was carried out after removing the applied load. Each test was standardized to a 20-second duration after reaching the maximum load, ensuring consistent testing conditions [27].

Specifically, hardness testing was executed at a load of 0.24N, performed at three distinct locations on the specimen's surface. In comparison to the intrinsic properties of the NiTi substrate, it is evident that the coatings have substantially enhanced the surface mechanical properties. Notably, the microhardness value increased from approximately 204VH for an uncoated NiTi sample to around 254 HV for a NiTi sample coated with sputtered Ta<sub>2</sub>O<sub>5</sub>. This marked improvement underscores the positive impact of Ta<sub>2</sub>O<sub>5</sub> coatings on the mechanical performance of the NiTi substrate.

*Corrosion Measurements*

In the realm of characterizing the corrosion behavior of NiTi alloys through in vitro experiments, a range of strategies has been employed. Initially, electrochemical experiments were conducted to assess electrochemical properties such as corrosion potential, polarization resistance, and passive current density. These properties were scrutinized due to their potential relevance to alloy biocompatibility [29].

Fig. 4a presents the results of the open circuit potential (OCP) test for NiTi samples coated

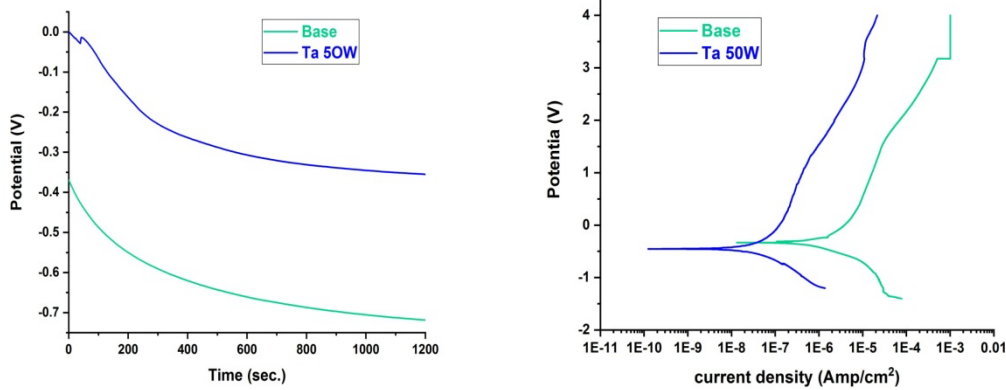


Fig. 4. The open circuit potential test and polarization curve (Tafel) for un-coated (base)NiTi alloy coated with Ta<sub>2</sub>O<sub>5</sub> films.

with Ta<sub>2</sub>O<sub>5</sub> compared to uncoated samples when exposed to artificial saliva (AS) solutions. Notably, the coated sample exhibited a substantial increase in passivation, with an OCP of -0.355 Volt, compared to -0.719 Volt for the uncoated sample.

Fig. 4b illustrates the polarization curve (Tafel) testing for Ta<sub>2</sub>O<sub>5</sub>-coated samples in contrast to uncoated samples. It is evident that the corrosion rate significantly decreases for the samples coated with Ta<sub>2</sub>O<sub>5</sub> compared to the uncoated base sample. Specifically, the corrosion rate for the Ta<sub>2</sub>O<sub>5</sub>-coated sample measures 1.803×10<sup>-4</sup> mmpy, while the uncoated sample records a corrosion rate of 7.146×10<sup>-3</sup> mmpy. This translates to a remarkable 39-fold reduction in the corrosion rate and a substantial enhancement in corrosion resistance. This heightened polarization resistance can be attributed to a thin, passive, and inert Ta<sub>2</sub>O<sub>5</sub> layer formed in the coating structure [30].

The protection efficiency can be determined from the equation below:

$$PE = \frac{i_{corr,uncoated} - i_{corr,coated}}{i_{corr,uncoated}} \times 100 \quad (1)$$

Where *i*<sub>corr, uncoated</sub> is the corrosion current for the uncoated sample and *i*<sub>corr, Coated</sub> is the corrosion current for the coated sample. The samples coated with Ta<sub>2</sub>O<sub>5</sub> achieved excellent protection efficiency, reaching 97.43%.

#### Bio-compatibility Tests

Biocompatibility tests were conducted by immersing the samples in synthetic simulated body fluid (SBF) for a duration of one month. Fig. 5 provides optical microscope images of the coated and uncoated NiTi samples after immersion in SBF. Remarkably, a layer of hydroxyapatite forms

on the surface of every sample, a crucial indicator of biocompatibility, as it indicates the material's ability to interact favorably with biological environments [31].

In the microscopy images for all the samples, there is a noticeable presence of agglomerated hydroxyapatite, particularly pronounced in the sample coated with Ta<sub>2</sub>O<sub>5</sub> (50W). This agglomeration highlights the effectiveness of Ta<sub>2</sub>O<sub>5</sub> in promoting the formation of hydroxyapatite layers.

Fig. 6 further underscores the biocompatibility of the samples by displaying the appearance of a distinctive hydroxyapatite peak at 2θ = 31.766, which closely matches the standard XRD pdf standard card ICDD 09-0432 for hydroxyapatite. Notably, this peak exhibits higher intensity than the previous samples, emphasizing the enhanced biocompatibility achieved with the Ta<sub>2</sub>O<sub>5</sub> coating.

Additionally, the XRD analysis reveals the presence of Ta<sub>2</sub>O<sub>5</sub> peaks at 2θ = 23.39, 26.47, and 36.49, in alignment with the standard XRD pdf card ICDD 21-1199 for tantalum oxide. This observation is attributed to the transformation of tantalum into tantalum oxide during the heat treatment of the samples. Overall, these findings collectively affirm the biocompatibility and effectiveness of the Ta<sub>2</sub>O<sub>5</sub> coating in facilitating the formation of hydroxyapatite layers, essential for the favorable interaction of the material with biological systems.

#### Ion Release Evaluation

This portion of the study addressed the concern of nickel ion release from NiTi substrates. To investigate this issue, we examined Ni ion release from NiTi substrate samples coated with

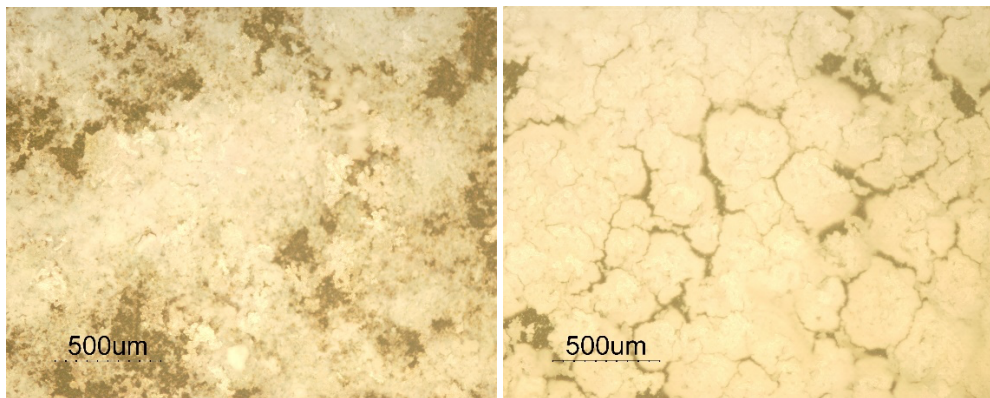


Fig. 5. Microscopy test images for samples after biocompatibility test, a: NiTi base, b: Ta<sub>2</sub>O<sub>5</sub> coated NiTi.

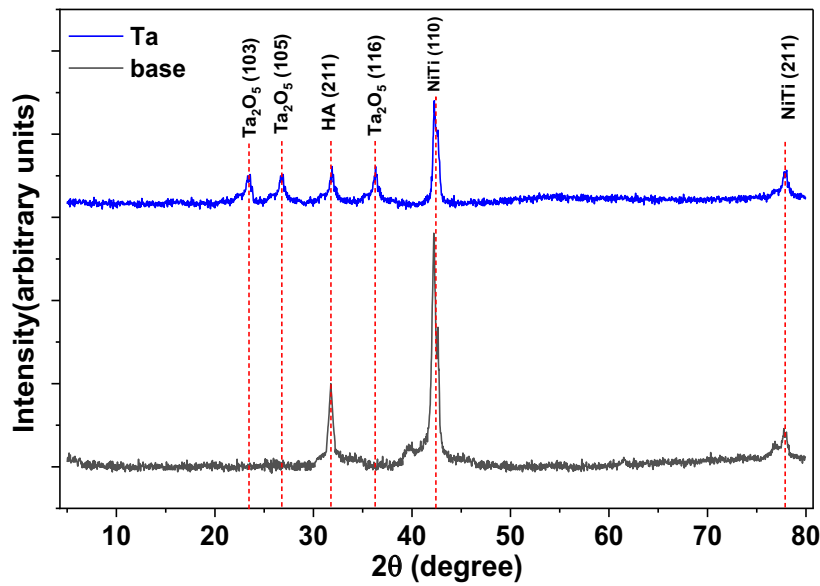


Fig 6. XRD pattern for a pattern for biocompatibility test of uncoated NiTi alloy samples coated with Ta<sub>2</sub>O<sub>5</sub> layer.

sputtered Ta<sub>2</sub>O<sub>5</sub> films when exposed to body fluids. The objective was to assess how effectively the sputtered coating prevented the out-diffusion of nickel ions from the substrate.

For this investigation, the samples were immersed statically in separate containers containing 100 ml of artificial saliva (AS) solution for a duration of 14 days. Following the corrosion test, the solutions collected from each sample were analyzed to determine the concentrations of nickel ions using Atomic Absorption Spectroscopy (AAS).

The results revealed that nickel ion release was 66.6 ppb for uncoated samples and 55.5 ppb for Ta<sub>2</sub>O<sub>5</sub>-coated NiTi samples immersed in the AS solution. Importantly, these values were well below the critical concentration range (600–2500 mg) known to trigger allergic reactions [32, 33]. This underscores that all NiTi substrate samples utilized in our study remained within clinically acceptable limits concerning the number of nickel ions released into the synthetic saliva, maintaining constant acidity.

Notably, the Ta<sub>2</sub>O<sub>5</sub> coating on the NiTi substrate samples appeared to act as an effective barrier, impeding the outward diffusion of metal ions from the bulk alloy. This suggests a promising avenue for mitigating the release of potentially allergenic nickel ions in biomedical applications.

## CONCLUSION

In this study, we conducted a comprehensive investigation into the coating of NiTi alloy substrates with nanostructured Ta<sub>2</sub>O<sub>5</sub> coatings using the DC reactive magnetron sputtering technique. The primary focus was to evaluate the resulting material's biological safety and its impact on the physical properties of the NiTi substrates, with a particular interest in its corrosion resistance and biocompatibility. Here, we delve into the detailed findings and implications of the study:

1. Coating Methodology: The study successfully employed the DC reactive magnetron sputtering technique to deposit nanostructured Ta<sub>2</sub>O<sub>5</sub> coatings onto NiTi alloy substrates. This technique allowed for precise control over the coating process, ensuring uniformity and adhesion.

2. Enhanced Corrosion Resistance: One of the study's key findings was the remarkable improvement in corrosion resistance observed in the Ta<sub>2</sub>O<sub>5</sub>-coated NiTi substrates. The passive Ta<sub>2</sub>O<sub>5</sub> layer acted as a robust barrier, preventing the out-diffusion of metal ions, particularly nickel, even when exposed to somewhat acidic artificial saliva. This enhanced corrosion resistance is a crucial characteristic for the long-term performance of biomedical implants and devices.

3. Reduced Nickel Ion Release: The study quantitatively assessed the release of nickel ions

from the coated and uncoated NiTi samples when immersed in artificial saliva. The results showed a substantial reduction in nickel ion release from the Ta<sub>2</sub>O<sub>5</sub>-coated samples, well below the critical concentration range known to induce allergic reactions. This demonstrated the biological safety of the coated NiTi substrates.

4. Nanostructured Ta<sub>2</sub>O<sub>5</sub> Thin Films: The study emphasized the quality of the nanostructured Ta<sub>2</sub>O<sub>5</sub> thin films deposited on the NiTi samples. These films exhibited uniformity and homogeneity, with surface roughness parameters such as average roughness (Ra) and root mean square roughness (Rq) well within acceptable ranges.

5. Biocompatibility: The coated NiTi samples demonstrated exceptional biocompatibility, as evidenced by the formation of hydroxyapatite layers on their surfaces when immersed in synthetic simulated body fluid. The agglomeration of hydroxyapatite was particularly pronounced in the Ta<sub>2</sub>O<sub>5</sub>-coated samples, highlighting their potential for favorable interaction with biological environments.

6. Medical Applications: The promising outcomes of this study suggest potential applications in the field of medicine, particularly in orthodontics. Coated NiTi materials, such as Orthodontic Archwires, could benefit from the enhanced corrosion resistance and biocompatibility provided by the Ta<sub>2</sub>O<sub>5</sub> coatings.

In conclusion, the successful coating of NiTi alloy substrates with nanostructured Ta<sub>2</sub>O<sub>5</sub> coatings using the DC reactive magnetron sputtering technique holds great promise for biomedical applications. The study confirms not only the biological safety of the coated materials but also significant improvements in their physical properties, making them suitable candidates for various medical and dental technologies.

#### CONFLICT OF INTEREST

The authors declare that there is no conflict of interests regarding the publication of this manuscript.

#### REFERENCES

1. Fernández-Lizárraga M, García-López J, Rodil SE, Ribas-Aparicio RM, Silva-Bermudez P. Evaluation of the Biocompatibility and Osteogenic Properties of Metal Oxide Coatings Applied by Magnetron Sputtering as Potential Biofunctional Surface Modifications for Orthopedic Implants. *Materials (Basel, Switzerland)*. 2022;15(15):5240.
2. Zhang S, Liu C, Zhao Z, Dong W, Zhang C, Zhang X, et al. Study on structural and optical properties of TiO<sub>2</sub> thin films prepared by sol-gel process. *Materials, Active Devices, and Optical Amplifiers*; 2004/05/12: SPIE; 2004.
3. Dai Z, Naramoto H, Narumi K, Yamaoto S. Epitaxial growth of rutile films on Si(100) substrates by thermal oxidation of evaporated titanium films in argon flux. *J Phys: Condens Matter*. 1999;11(43):8511-8516.
4. Leprince-Wang Y, Yu-Zhang K. Study of the growth morphology of TiO<sub>2</sub> thin films by AFM and TEM. *Surf Coat Technol*. 2001;140(2):155-160.
5. Huang AP, Chu PK, Wang L, Cheung WY, Xu JB, Wong SP. Fabrication of rutile TiO<sub>2</sub> thin films by low-temperature, bias-assisted cathodic arc deposition and their dielectric properties. *J Mater Res*. 2006;21(4):844-850.
6. Peng X, Wang J, Thomas DF, Chen A. Tunable growth of TiO<sub>2</sub> nanostructures on Ti substrates. *Nanotechnology*. 2005;16(10):2389-2395.
7. Chong LH, Mallik K, Groot CHd, Kersting R. The structural and electrical properties of thermally grown TiO<sub>2</sub> thin films. *J Phys: Condens Matter*. 2005;18(2):645-657.
8. Kasikov A, Aarik J, Mändar H, Moppel M, Pärs M, Uustare T. Refractive index gradients in TiO<sub>2</sub> thin films grown by atomic layer deposition. *J Phys D: Appl Phys*. 2005;39(1):54-60.
9. Choi BJ, Jeong DS, Kim SK, Rohde C, Choi S, Oh JH, et al. Resistive switching mechanism of TiO<sub>2</sub> thin films grown by atomic-layer deposition. *J Appl Phys*. 2005;98(3).
10. Khalaf MK, Hassan NK, Khudiar AI, Salman IK. Photoconductivities of Nanocrystalline Vanadium Pentoxide Thin Film Grown by Plasma RF Magnetron Sputtering at Different Conditions of Deposition. *Physics of the Solid State*. 2020;62(1):74-82.
11. Hamil MI, Khalaf MK, Al-Shakban M. MAGNETRON SPUTTERED NANOCRYSTALLINE TiN THIN FILMS AND CORROSION PROPERTIES. *Periódico Tchê Química*. 2020;17(35):164-173.
12. Hamil M, Siyah M, Khalaf M. Electrophoretic deposition of Thin film TiO<sub>2</sub> on Ti6AL4V alloy surface for biomedical applications. *Egyptian Journal of Chemistry*. 2020;0(0):0-0.
13. Zhou X-S, Lin Y-H, Li B, Li L-J, Zhou J-P, Nan C-W. Processing and characterization of TiO<sub>2</sub> film prepared on glass via pulsed laser deposition. *J Phys D: Appl Phys*. 2006;39(3):558-562.
14. Gracia F, Yubero F, Holgado JP, Espinos JP, Gonzalez-Elipe AR, Girardeau T. SiO<sub>2</sub>/TiO<sub>2</sub> thin films with variable refractive index prepared by ion beam induced and plasma enhanced chemical vapor deposition. *Thin Solid Films*. 2006;500(1-2):19-26.
15. Subramanian NS, Santhi B, Veeraganesh V, Vinoth C, Murugan G, Subbaraj GK. Studies on evaporated titanium oxide thin films for oxygen gas detection. *Ionics*. 2004;10(1-2):56-62.
16. Hou Y-Q, Zhuang D-M, Zhang G, Zhao M, Wu M-S. Influence of annealing temperature on the properties of titanium oxide thin film. *Appl Surf Sci*. 2003;218(1-4):98-106.
17. Szczyrbowski J, Bräuer G, Ruske M, Bartella J, Schroeder J, Zmelty A. Some properties of TiO<sub>2</sub> layers prepared by medium frequency reactive sputtering. *Surf Coat Technol*. 1999;112(1-3):261-266.
18. Baba K, Hatada R. Synthesis and properties of TiO<sub>2</sub> thin films by plasma source ion implantation. *Surf Coat Technol*. 2001;136(1-3):241-243.
19. Wang H, Wang T, Xu PEI. *Journal of Materials Science: Materials in Electronics*. 1998;9(5):327-330.



20. Zwölf Jahre – Bilanz und Ausblick. *Der Freie Zahnarzt*. 2016;60(10):20-20.
21. Newman DM, Wears ML, Jollie M, Choo D. Fabrication and characterization of nano-particulate PtCo media for ultra-high density perpendicular magnetic recording. *Nanotechnology*. 2007;18(20):205301.
22. Jelle BP, Hynd A, Gustavsen A, Arasteh D, Goudey H, Hart R. Fenestration of today and tomorrow: A state-of-the-art review and future research opportunities. *Sol Energy Mater Sol Cells*. 2012;96:1-28.
23. Wu S-j, Hong B, Huang B-s. Effect of growth and annealing temperatures on crystallization of tantalum pentoxide thin film prepared by RF magnetron sputtering method. *J Alloys Compd*. 2009;475(1-2):488-493.
24. Chen J, Suwardy J, Subramani T, Jevasuwan W, Takei T, Toko K, et al. Control of grain size and crystallinity of poly-Si films on quartz by Al-induced crystallization. *CrystEngComm*. 2017;19(17):2305-2311.
25. Chan KY, Teo BS. Effect of Ar pressure on grain size of magnetron sputter-deposited Cu thin films. *IET Science, Measurement & Technology*. 2007;1(2):87-90.
26. Parizek NJ, Steines BR, Haque E, Altmaier R, Adamcakova-Dodd A, O'Shaughnessy PT, et al. Acute in vivo pulmonary toxicity assessment of occupationally relevant particulate matter from a cellulose nanofiber board. *NanoImpact*. 2020;17:100210.
27. Shahzad A, Saeed H, Iqtedar M, Hussain SZ, Kaleem A, Abdullah R, et al. Size-Controlled Production of Silver Nanoparticles by *Aspergillus fumigatus* BTCB10: Likely Antibacterial and Cytotoxic Effects. *Journal of Nanomaterials*. 2019;2019:1-14.
28. Firouzabadi SS, Dehghani K, Naderi M, Mahboubi F. Numerical investigation of sputtering power effect on nano-tribological properties of tantalum-nitride film using molecular dynamics simulation. *Appl Surf Sci*. 2016;367:197-204.
29. Hu T, Chu C, Xin Y, Wu S, Yeung KWK, Chu PK. Corrosion products and mechanism on NiTi shape memory alloy in physiological environment. *J Mater Res*. 2010;25(2):350-358.
30. Firouzabadi SS, Naderi M, Dehghani K, Mahboubi F. Effect of nitrogen flow ratio on nano-mechanical properties of tantalum nitride thin film. *J Alloys Compd*. 2017;719:63-70.
31. García C, Ceré S, Durán A. Bioactive coatings prepared by sol-gel on stainless steel 316L. *Journal of Non-Crystalline Solids*. 2004;348:218-224.
32. Schroeder HA, Balassa JJ, Tipton IH. Abnormal trace metals in man — nickel. *J Chronic Dis*. 1962;15(1):51-65.
33. Barrett RD, Bishara SE, Quinn JK. Biodegradation of orthodontic appliances. Part I. Biodegradation of nickel and chromium in vitro. *Am J Orthod Dentofacial Orthop*. 1993;103(1):8-14.